Optimal Power Flow Based on Novel Multi-objective Artificial Fish Swarm Algorithm

Gang Guo, Jie Qian*, and Shuaiyong Li

Abstract—**Computer technology provides new possibilities for handling the many-objective optimal power flow (MOOPF) problems with high-dimension and non-differentiability. As one of typical intelligent algorithms, the novel multi-objective artificial fish swarm algorithm (NMAFSA) is proposed to solve the MOOPF problems and realize the economical operation of power systems. The NMAFSA algorithm, which combines with optimal solution guidance (OSG) principle and non-inferior retention (NIR) mechanism, is effective to reduce the fuel cost, emission and power loss. Compared with the representative many-objective particle swarm optimization (MPSO) and non-dominated sorting genetic algorithm-II (NSGA-II), the superiority and adaptability of presented NMAFSA algorithm are validated. Six simulation trials are carried out on MATLAB software, including the dual-objective and triple-objective optimizations on three different scale power systems. Detailed results demonstrate that the suggested NMAFSA algorithm with stable-operation and fast-convergence has great potential to deal with the MOOPF problems more efficiently. Furthermore, the generation distance (GD) index also quantitatively proves that the NMAFSA algorithm can obtain the well-distributed Pareto front (PF).**

Index Terms—**Artificial fish swarm algorithm, Optimal power flow, Computer technology, Generation distance**

I. Introduction

THE reasonable adjustment of controllable variables can optimize the running state of power system, which is helpful to achieve the operational safety and economical efficiency. As an essential method, the optimal power flow (OPF) is widely used in the economic dispatch of power system [1-3]. Besides, the many-objective OPF (MOOPF) problems, which consider the power loss, fuel cost and exhaust emission simultaneously, can evaluate the operation state of electric system more comprehensively.

However, traditional methods are unsuitable for solving MOOPF problems due to the non-convexity and non-linearity characteristics. Intelligent algorithm, a widely-applied computer technology, plays an important role in handling the high-dimensional MOOPF problems. For example, the efficient meta-heuristic algorithm [4], the quasi-oppositional cuckoo search algorithm [5] and the improved strength Pareto evolutionary algorithm [6] have successfully solved the MOOPF problems.

Artificial fish swarm algorithm (AFSA) with parallel processing capabilities can handle various practical problems such as the industrial problems [7] and the well trajectory optimization [8]. In this paper, taking the AFSA algorithm as main body and integrating the classification processing strategy to generate the proposed novel multi-objective AFSA (NMAFSA) algorithm. To escape from the local optimal solution and improve the optimization efficiency, the optimal solution guidance (OSG) principle and non-inferior retention (NIR) mechanism are integrated into the presented NMAFSA algorithm.

Based on MATLAB software, six MOOPF trials which aim to reduce the fuel cost, emission and power loss are solved by the suggested NMAFSA algorithm. In detail, the significant advantages of NMAFSA algorithm in dealing with MOOPF problems are powerfully validated by comparing with the many-objective particle swarm optimization (MPSO) which is one of the most popular algorithms and the non-dominated sorting genetic algorithm-II (NSGA-II) which is usually adopted as the performance evaluation benchmark.

II. MOOPF Model

The model of security-constrained MOOPF problem shown as (1) ~ (3) is formed by the optimization goals (*OG*s), equality restrictions (*ER*s) and inequality ones (*IR*s).

$$F_{OG} = (OG_1, \cdots, OG_i, \cdots, OG_W) \tag{1}$$

$$ER_{(k)} = 0, \quad k = 1, 2, \cdots, h \tag{2}$$

$$IR_{(j)} \le 0, \quad j = 1, 2, \cdots, g \tag{3}$$

where OG_i is the ith goal and W is the number of simultaneously-optimized objectives. h and g, respectively, indicate the numbers of *ER*s and *IR*s.

A. OGs

The exhaust emissions (F_{EM}), quadratic fuel cost (F_{BF}) and active power loss (F_{AP}) are studied in this paper. Besides, the fuel cost with valve-point effect (F_{FV}) is also considered to further evaluate the performance of NMAFSA algorithm.

► F_{EM} (ton/h)

$$F_{EM} = \sum_{i=1}^{N_G} [\alpha_i P_{Gi}^2 + \beta_i P_{Gi} + \gamma_i + \eta_i \exp(\lambda_i P_{Gi})] \tag{4}$$

► F_{BF} (\$/h)

Manuscript received November 28, 2019; revised April 3, 2020. This work was supported the National Natural Science Foundation Project of China (No.61703066), Natural Science Foundation Project of Chongqing (No.cstc2018jcyjAX0536).

Gang Guo is with the School of Information Technology, Luoyang Normal University, Luoyang, Henan 471934, China (e-mail: guogangchina @sina.cn).

Jie Qian is with the Key Laboratory of Complex Systems and Bionic Control, Chongqing University of Posts and Telecommunications, Chongqing 400065, China (corresponding author, Tel: 13618344186; e-mail: qianjie@126.com).

Shuaiyong Li is with the Key Laboratory of Industrial Internet of Things & Networked Control, Ministry of Education, Chongqing University of Posts and Telecommunications, Chongqing 400065, China (e-mail: lishuaiyong@cqupt.edu.cn).

$$F_{BF}=\sum_{i=1}^{N_G}(a_i+b_iP_{Gi}+c_iP_{Gi}^2) \quad (5)$$

► F_{AP} (MW)

$$F_{AP}=\sum_{k=1}^{N_L}c_k[V_i^2+V_j^2-2V_iV_j\cos(\delta_i-\delta_j)] \quad (6)$$

► F_{FV} ($/h)

$$F_{FV}=\sum_{i=1}^{N_G}(a_i+b_iP_{Gi}+c_iP_{Gi}^2+\left|d_i\times\sin(e_i\times(P_{Gi}^{\min}-P_{Gi}))\right|) \quad (7)$$

where N_G and N_L are the numbers of generators and transmission lines. The other mentioned symbols can refer to references [9-11].

B. ERs

The active power balance equation (8) and the reactive one (9) constitute two *ER*s of MOOPF problems [9, 12-14].

$$P_{Gi}-P_{Di}-V_i\sum_{j\in N_i}V_j(G_{ij}\cos(\delta_i-\delta_j)+B_{ij}\sin(\delta_i-\delta_j))=0 \quad (8)$$
$$i\in N$$

$$Q_{Gi}-Q_{Di}-V_i\sum_{j\in N_i}V_j(G_{ij}\sin(\delta_i-\delta_j)-B_{ij}\cos(\delta_i-\delta_j))=0 \quad (9)$$
$$i\in N_{PQ}$$

where N and N_{PQ} indicate the amount of system-nodes (except the slack one) and *PQ* nodes.

The *ER*s are used as the termination condition of Newton Raphson method. The acquisition of power flow solutions that do not violate any constraints naturally indicates that the *ER*s are satisfied.

C. IRs

Macroscopically, *IR*s can be divided into the constraints on independent variables and dependent ones.

1) IRs on Independent Variables

The independent variables include: 1) generator node voltage V_G, 2) generator active power output at *PV* node P_G, 3) tap ratios of transformer T, 4) reactive power injection Q_C [9, 14, 15]. The *IR*s on V_G, P_G, T and Q_C are shown as (10) ~ (13).

$$V_{Gi}^{\min}\le V_{Gi}\le V_{Gi}^{\max}, i\in N_G \quad (10)$$

$$P_{Gi}^{\min}\le P_{Gi}\le P_{Gi}^{\max}, i\in N_G (i\ne 1) \quad (11)$$

$$T_i^{\min}\le T_i\le T_i^{\max},\ i\in N_T \quad (12)$$

$$Q_{Ci}^{\min}\le Q_{Ci}\le Q_{Ci}^{\max},\ i\in N_C \quad (13)$$

where N_T and N_C are the numbers of transformers and compensators.

2) IRs on Dependent Variables

The dependent variables include: 1) load node voltage V_L, 2) generator active power at slack node P_{G1}, 3) generator reactive power Q_G, 4) apparent power of transmission line S [9, 14]. The *IR*s on V_L, P_{G1}, Q_G and S are shown as (14) ~ (17).

$$V_{Li}^{\min}\le V_{Li}\le V_{Li}^{\max},\ i\in N_{PQ} \quad (14)$$

$$P_{G1}^{\min}\le P_{G1}\le P_{G1}^{\max} \quad (15)$$

$$Q_{Gi}^{\min}\le Q_{Gi}\le Q_{Gi}^{\max},\ i\in N_G \quad (16)$$

$$S_l^{\max}-S_l\ge 0,\ l\in N_L \quad (17)$$

D. IRs Processing

The practicable power flow solutions obtained by NMAFSA algorithm should meet all system restrictions. Therefore, adopting the appropriate treatment of *IR*s is very important to solve the MOOPF problems. In this paper, the elite dominant strategy with violation-consideration (EDSV) is proposed to pick out high-quality Pareto optimal set (POS).

Firstly, the dominant relationship of two different solutions is clarified based on the *IR* violation (IR_{vio}) and *OG* values. It can be determined that the S_1 solution is better than S_2 whether condition (18) or (19) is satisfied.

$$IR_{vio}(S_1)<IR_{vio}(S_2) \quad (18)$$

$$\begin{cases} IR_{vio}(S_1)=IR_{vio}(S_2) \\ OG_i(S_1)\le OG_i(S_2),\forall i\in\{1,2,...,W\} \\ OG_j(S_1)<OG_j(S_2),\exists j\in\{1,2,...,W\} \end{cases} \quad (19)$$

Besides the R_{ank} index which can be determined by (18) and (19), the crowding distance (C_{dis}) index is also used to judge the quality of two solutions with the same R_{ank} index. The C_{dis} is defined as formula (20) [9, 16-18].

$$C_{dis}(i)=\sum_{j=1}^{N}\frac{OG_j(i-1)-OG_j(i+1)}{OG_j^{\max}-OG_j^{\min}} \quad (20)$$

where N is the size of POS. The OG_j^{max} and OG_j^{min} indicate the largest and smallest values of the jth goal.

The ranking strategy in this paper is inspired by the non-inferior ranking method [16, 19, 20]. When determining the final POS set, the solutions with smaller R_{ank} are preferred, followed by the solutions with larger C_{dis}. The selection principle can be summed up as formulas (21) and (22).

$$R_{ank}(S_1)<R_{ank}(S_2) \quad (21)$$

$$\begin{cases} R_{ank}(S_1)=R_{ank}(S_2) \\ C_{dis}(S_1)>C_{dis}(S_2) \end{cases} \quad (22)$$

Based on R_{ank} and C_{dis} indicators, the flowchart of seeking satisfactory POS by proposed EDSV strategy is summarized as Fig. 1. Worthy of note is that, the candidate solution (CANS) set consists of the N solutions from the previous iteration and the N randomly-generated solutions.

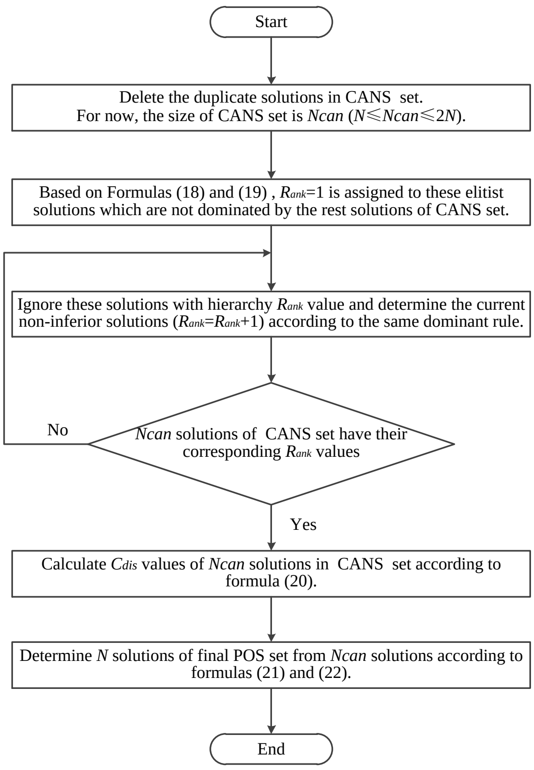

Fig.1 Flowchart of seeking POS set

III. NMAFSA ALGORITHM

The preponderance of NMAFSA algorithm on MOOPF problems is verified by taking the MPSO and NSGA-II as two comparing algorithms. The applications of MPSO method on MOOPF problems can refer to literatures [9, 11] while the NSGA-II method can refer to literatures [21, 22].

The artificial fish swarm (AFSA) algorithm has good randomness, which has been widely concerned by many scholars [23-25]. However, when solving the MOOPF problems with non-convex feature, the basic AFSA algorithm with poor-performance is easy to be trapped by local optimums. Therefore, the OSG guidance and NIR retention strategies are proposed to generate the novel NMAFSA algorithm with better performance.

A. OSG Guidance Strategy

Different from the traditional AFSA algorithm, the foraging, clustering and random behavior of the proposed NMAFSA algorithm are based on the non-inferior layering mechanism. In this paper, the non-inferior layering mechanism defines the top ζ_1% of POS set as the superior fish population and the bottom ζ_2% as the inferior one. Specifically, the superior fish population engaged in foraging behavior while and the inferior population engaged in clustering behavior. The rest fish population adopts the randomly-updated way. Besides, both random and clustering behaviors are modified by OSG guidance strategy.

► Foraging

$$YPos(i) = Pos(i) + \frac{\beta_1 * \delta_{step}(Pos(j) - Pos(i))}{\| Pos(j) - Pos(i) \|} \tag{23}$$
$$i = 1, 2, \cdots, \varsigma_1 \% * N$$

► Random behavior

$$YPos(i) = Pos(i) + \omega * (Pos_{best} - Pos(i)) \tag{24}$$
$$i = (\varsigma_1 \% * N + 1), (\varsigma_1 \% * N + 2), \cdots, (1 - \varsigma_2 \%) * N$$

► Clustering

$$YPos(i) = Pos(i) + \frac{\beta_2 * (Pos_{best} - Pos(i))}{\| Pos_{best} - Pos(i) \|} \tag{25}$$
$$i = ((1 - \varsigma_2 \%)*N + 1), ((1 - \varsigma_2 \%)*N + 2), \cdots, N$$

where $Pos(i)$ represents the position of the ith fish, that is, the control variable set of the ith power flow solution. The δ_{step} indicates the moving step parameter while ω ($\omega \in (0,1)$) is the weight coefficient of random behavior. The β_1 and β_2 (β_1, β_2 $\in$ (0,1)) are two random-number arrays while Pos_{best} represents the position of current optimal fish.

The clustering and random behaviors based on OSG guidance mechanism can accelerate the speed of fish population approaching the best solution and improve the efficiency of NMAFSA algorithm.

B. NIR Retention Strategy

After each location-updating based on foraging, random and clustering operations, the presented NIR retention strategy is used to verify the validity of current update. The proposed NMAFSA algorithm only keeps the better position which is superior to the current one. Otherwise, the current position remains unchanged. The NIR strategy is summarized as formula (26) and the dominant relationship of two fish individuals is clarified according to formulas (18) and (19).

$$Pos(i+1) = \begin{cases} YPos(i), \ if \ YPos(i) \text{ dominates } Pos(i) \\ Pos(i), \qquad otherwise \end{cases} \tag{26}$$

C. NMAFSA Algorithm on MOOPF Problem

The NMAFSA algorithm, which extends single-objective optimization to multi-objective one, has great potential to solve the MOOPF problems. Table I shows the main steps for handling MOOPF problems by the suggested NMAFSA algorithm.

IV. PARAMETERS AND SYSTEMS

The effects of maximum iteration number (ite_{max}) and different population size on the performance of NMAFSA algorithm are studied. This section also gives the detailed parameters of NMAFSA algorithm and three involved standard systems.

A. Parameters

The simulation case which simultaneously minimizes F_{EM} and F_{BF} on IEEE 30-bus system is used to determine a feasible parameter-combination set. Fig. 2 gives the Pareto fronts (PFs) obtained by NMAFSA method with different ite_{max}, which states that ite_{max}=300 and 400 find the uniformly-distributed PFs. Due to their similar optimization performance, ite_{max} =300 is adopted in these cases on IEEE 30-bus system considering the reduction of running time.

TABLE I
MAIN STEPS OF NMAFSA METHOD ON MOOPF PROBLEMS

input: the parameters of NMAFSA algorithm and the initial CANS set
begin
ite=1
while $ite < ite_{max}$
Perform the power flow calculation on the initial fish population and determine the current POS according to Fig. 1.
for i=1,2,…,0.01*ζ_1*N
Update the position of superior population based on formula (23);
Retain the non-inferior individuals according to NIR strategy;
end for
for i=0.01*ζ_1*N+1, 0.01*ζ_1*N+2,…,(1-ζ_2%)*N
Perform the random update operation based on formula (24);
Retain the non-inferior individuals according to NIR strategy;
end for
for i=(1-ζ_2%)*N+1, (1-ζ_2%)*N+2,…,N
Update the position of inferior fish population based on formula (25);
Retain the non-inferior individuals according to NIR strategy;
end for
Determine the current POS;
ite=ite+1;
Generate new CANS set;
end while
end
output: the ultimate POS

Besides, Fig. 3 gives the PFs determined by NMAFSA method and it clearly indicates that NMAFSA algorithm can obtain the satisfactory PFs with different population size.

The other parameters of NMAFSA method are set as: ζ_1=ζ_2=20, N=50, δ_{step}=0.3, ite_{max}=300 (IEEE 30-bus system), ite_{max}=500 (IEEE 57-bus and 118-bus systems). In addition, each objective-combination trial is carried out 30 times independently.

B. *Systems*

Three power systems with different scales are used to validate the applicability of MPSO, NSGA-II and NMAFSA algorithms in dealing with the dual-objective and tri-objective MOOPF problems.

The structures of IEEE 30-bus and 57-bus systems are given in literatures [9, 18, 26]. The IEEE 30-bus system includes 24-dimensional control variables and IEEE 57-bus system includes 33-dimensional ones. The transformer taps are both limited within [0.9 1.1] p.u.. The shunt capacitors of 30-bus and 57-bus system, respectively, are limited within [0 0.05] p.u and [0 0.3] p.u.. The emission coefficients and other details are clarified in [6, 9, 27].

The MOOPF problem on complex IEEE 118-bus system with 128-dimensional control variables is also discussed to comprehensively evaluate the performance of NMAFSA algorithm. The structure and details can be found in [11, 18].

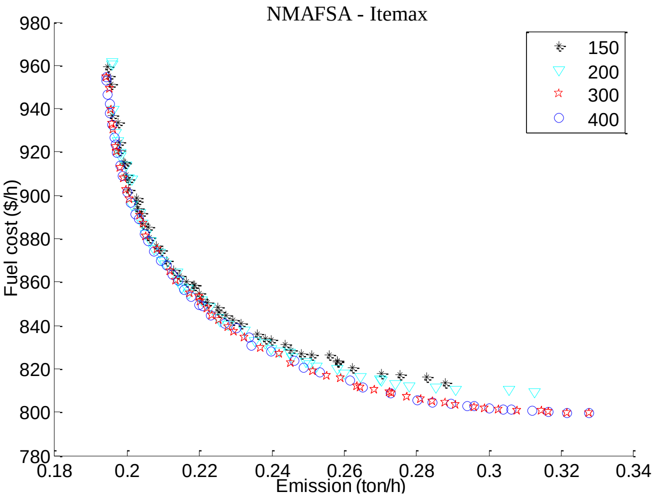

Fig.2 PFs with different ite_{max}

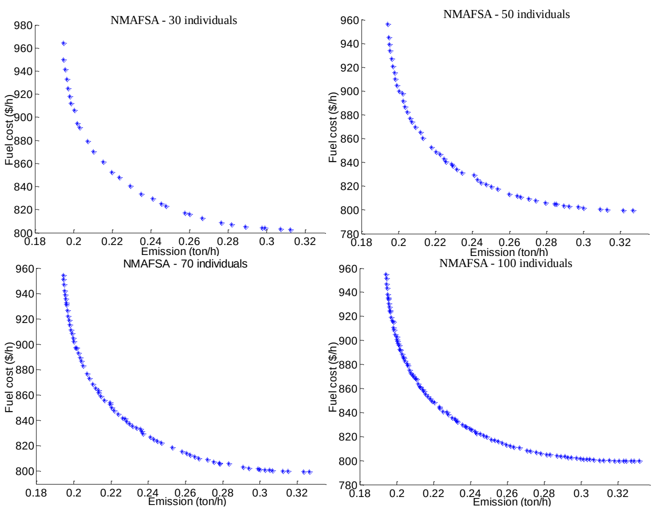

Fig.3 PFs with different population-size

V. Cases and Results

Six simulation cases on three different-scale systems are studied in this paper.

A. *Trials on IEEE 30-bus System*

Two dual-goal and one triple-goal MOOPF cases are performed on the standard 30-bus system. In detail, *Exp* 1 aims to optimize F_{BF} and F_{EM}, *Exp* 2 aims to optimize F_{FV} and F_{EM}, *Exp* 3 aims to optimize F_{BF}, F_{EM} and F_{AP} concurrently.

1) *Exp 1*

Fig. 4 shows the PFs obtained by NMAFSA and two comparison algorithms while TABLE II gives the details of best compromise solutions (BCSs). Fig.4 clearly indicates that MPSO method finds the worst PF while NMAFSA algorithm achieves the more advantageous one. The BCS of presented NMAFSA algorithm is composed of 0.2351 of F_{EM} and 830.79 of F_{BF}, which dominates the ones of MPSO and NSGA-II methods. TABLE II also gives the comparative result of other literature and it shows that the BCS of NMAFSA is better than the one of NHBA algorithm which includes 0.2375 of F_{EM} and 832.65 of F_{BF}.

2) *Exp 2*

Fig. 5 and TABLE III, respectively, give the PFs found by three mentioned algorithms and the details of obtained BCSs. Fig. 5 states that NMAFSA algorithm obtains the superior PF with better distribution although three methods have similar solution-diversity. TABLE III shows that the BCS of NMAFSA algorithm which consists of 0.2579 of F_{EM} and 855.83 of F_{FV} is more preferable than the ones of MOPSO and NSGA-II approaches.

TABLE II
BCS Solutions of *Exp* 1

independent variables	NSGA-II	MPSO	NMAFSA	NHBA [11]
P_{G2}(MW)	59.9725	61.0325	55.3090	58.1990
P_{G5}(MW)	22.9205	26.1819	26.9629	25.6741
P_{G8}(MW)	34.5538	34.9571	34.1204	27.0218
P_{G11}(MW)	28.1903	25.5818	26.1740	26.3626
P_{G13}(MW)	24.7072	24.3085	27.6256	31.3704
V_{G1}(p.u.)	1.0054	1.0875	1.0992	1.1000
V_{G2}(p.u.)	0.9930	1.0786	1.0910	1.0890
V_{G5}(p.u.)	0.9738	1.0560	1.0578	1.0537
V_{G8}(p.u.)	0.9973	1.0621	1.0762	1.0639
V_{G11}(p.u.)	1.0553	1.0841	1.0984	1.0880
V_{G13}(p.u.)	1.0882	1.0734	1.0791	1.0517
T_{11}(p.u.)	0.9834	1.0215	1.0686	1.0711
T_{12}(p.u.)	0.9376	1.0518	0.9160	0.9304
T_{15}(p.u.)	0.9677	0.9435	1.0299	1.1000
T_{36}(p.u.)	0.9430	1.0428	0.9864	1.0097
Q_{C10}(p.u.)	0.0234	0.0082	0.0387	0.0299
Q_{C12}(p.u.)	0.0167	0.0000	0.0288	0.0473
Q_{C15}(p.u.)	0.0059	0.0137	0.0119	0.0157
Q_{C17}(p.u.)	0.0077	0.0493	0.0441	0.0450
Q_{C20}(p.u.)	0.0301	0.0066	0.0476	0.0291
Q_{C21}(p.u.)	0.0097	0.0124	0.0108	0.0333
Q_{C23}(p.u.)	0.0023	0.0044	0.0312	0.0500
Q_{C24}(p.u.)	0.0286	0.0500	0.0137	0.0235
Q_{C29}(p.u.)	0.0208	0.0416	0.0300	0.0088
F_{EM} (ton/h)	0.2379	0.2352	**0.2351**	0.2375
F_{BF} ($/h)	833.19	831.32	**830.79**	832.65

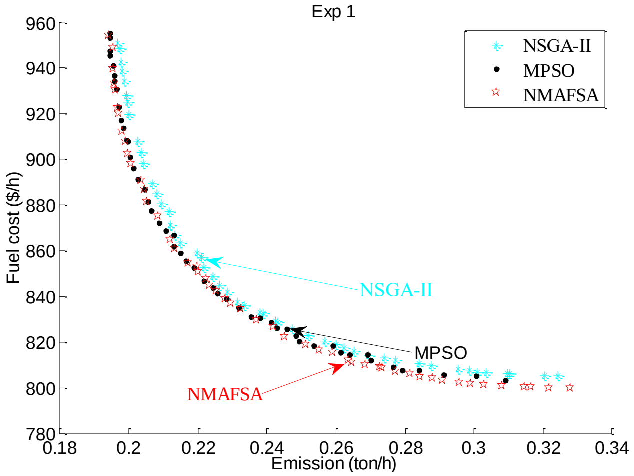

Fig.4 PFs of *Exp* 1

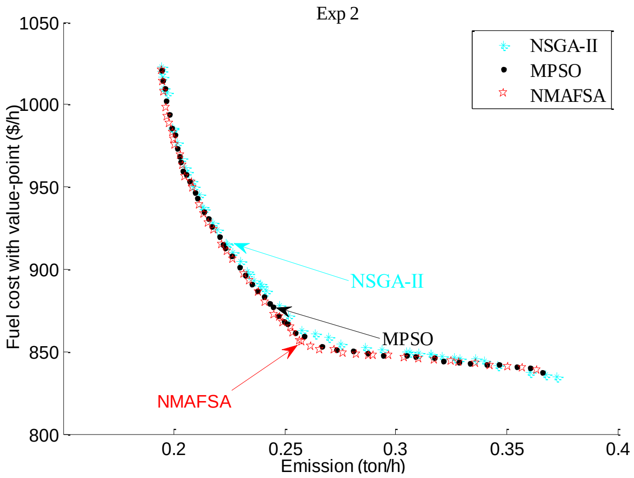

Fig.5 PFs of *Exp* 2

TABLE III
BCS SOLUTIONS OF *EXP* 2

independent variables	NSGA-II	MPSO	NMAFSA
P_{G2}(MW)	60.8395	51.8749	62.3020
P_{G5}(MW)	23.7605	22.9111	25.9040
P_{G8}(MW)	21.9856	34.6631	32.9081
P_{G11}(MW)	28.3491	18.4797	16.3379
P_{G13}(MW)	17.0558	25.7165	18.8095
V_{G1}(p.u.)	1.0587	1.0997	1.0923
V_{G2}(p.u.)	1.0373	1.0893	1.0805
V_{G5}(p.u.)	1.0132	1.0427	1.0649
V_{G8}(p.u.)	1.0126	1.0667	1.0635
V_{G11}(p.u.)	1.0521	1.0767	1.0690
V_{G13}(p.u.)	0.9817	1.0530	1.0865
T_{11}(p.u.)	0.9894	1.0778	1.0327
T_{12}(p.u.)	0.9654	0.9073	0.9146
T_{15}(p.u.)	1.0185	0.9694	1.0335
T_{36}(p.u.)	0.9473	1.0512	0.9835
Q_{C10}(p.u.)	0.0145	0.0000	0.0290
Q_{C12}(p.u.)	0.0079	0.0117	0.0091
Q_{C15}(p.u.)	0.0000	0.0086	0.0380
Q_{C17}(p.u.)	0.0237	0.0299	0.0255
Q_{C20}(p.u.)	0.0241	0.0500	0.0476
Q_{C21}(p.u.)	0.0318	0.0070	0.0254
Q_{C23}(p.u.)	0.0430	0.0000	0.0438
Q_{C24}(p.u.)	0.0427	0.0051	0.0500
Q_{C29}(p.u.)	0.0298	0.0345	0.0353
F_{EM} (ton/h)	0.2638	0.2586	**0.2579**
F_{FV} ($/h)	860.96	859.28	**855.83**

3) Exp 3

A triple-objective experiment (*Exp* 3), which considers the simultaneous optimization of F_{EM}, F_{BF} and F_{AP}, requires higher performance of suggested NMAFSA algorithm. The PFs of NSGA-II and NMAFSA algorithms are shown in Fig. 6 while the PFs of MPSO and NMAFSA are shown in Fig. 7. Both MPSO and NMAFSA algorithms achieves the uniformly-distributed and well-diversified PFs in contrast to NSGA-II algorithm. Furthermore, the PF of novel NMAFSA method is more superior to the one of MPSO algorithm.

Besides, the details of obtained BCSs of *Exp* 3 are given in TABLE IV. The BCS of proposed NMAFSA algorithm consists of 865.39 of F_{BF}, 4.3553 of F_{AP} and 0.2128 of F_{EM}, which surpasses the BCS of NSGA-II including 872.74 of F_{BF}, 4.8843 of F_{AP}, 0.2130 of F_{EM} . Furthermore, the BCS of NMAFSA algorithm is superior to the BCS of MPSO including 873.45 of F_{BF}, 4.6347 of F_{AP}, 0.2137 of F_{EM} as well. Additionally, NMAFSA algorithm also achieves the smaller F_{BF} and F_{EM} values comparing with MOFA-PFA algorithm in literature [28].

B. Trials on IEEE 57-bus System

One dual-objective case (*Exp* 4) and another triple one (*Exp* 5) are carried out on the standard 57-bus system. In detail, *Exp* 4 aims to optimize F_{BF} and F_{EM} at the same time. Meanwhile, *Exp* 5 aims to optimize F_{BF}, F_{EM} and F_{AP} synchronously.

1) Exp 4

Fig. 8 gives the PFs determined by NMAFSA algorithm and two comparison approaches while TABLE V gives the details of BCSs for *Exp* 4.

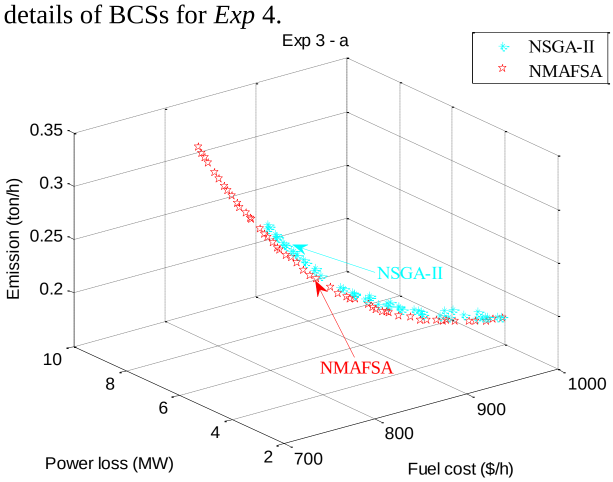

Fig.6 PFs of NSGA-II and NMAFSA for *Exp* 3

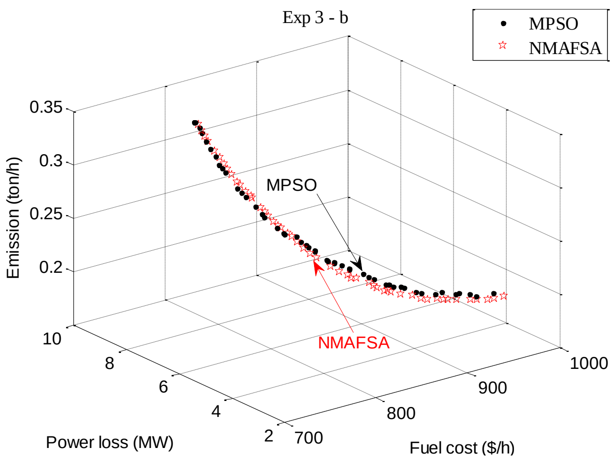

Fig.7 PFs of MPSO and NMAFSA for *Exp* 3

Fig. 8 intuitively indicates that NMAFSA algorithm achieves the significantly superior PF with satisfactory diversity in contrast to MPSO and NSGA-II methods. Besides, the BCS achieved by NMAFSA algorithm composed of 43114.71 of F_{BF} and 1.2421 of F_{EM} is better than the ones found by two comparative methods as well. To be more persuasive, the BCS of proposed NMAFSA algorithm also precedes the one of MODFA algorithm which is given in literature [18].

TABLE IV
BCS SOLUTIONS OF *EXP* 3

independent variables	NSGA-II	MPSO	NMAFSA	MOFA-PFA [28]
P_{G2}(MW)	80.0000	58.1879	60.9741	57.890
P_{G5}(MW)	28.0558	41.6045	36.8206	36.290
P_{G8}(MW)	35.0000	31.3610	33.6751	35.000
P_{G11}(MW)	26.7647	28.7171	27.6888	29.271
P_{G13}(MW)	31.3583	30.4097	32.6088	40.000
V_{G1}(p.u.)	1.1000	1.0810	1.0967	1.0985
V_{G2}(p.u.)	1.0933	1.0757	1.0886	1.0869
V_{G5}(p.u.)	1.0876	1.0553	1.0659	1.0625
V_{G8}(p.u.)	1.0933	1.0452	1.0760	1.0767
V_{G11}(p.u.)	1.0616	1.0462	1.0952	1.0857
V_{G13}(p.u.)	1.0997	1.0240	1.0792	1.0386
T_{11}(p.u.)	1.0877	0.9374	0.9952	1.0860
T_{12}(p.u.)	0.9831	0.9686	1.0528	0.9930
T_{15}(p.u.)	0.9688	1.0042	1.0664	1.0520
T_{36}(p.u.)	1.0356	0.9711	0.9783	1.0770
Q_{C10}(p.u.)	0.0000	0.0381	0.0462	0.0140
Q_{C12}(p.u.)	0.0075	0.0293	0.0112	0.0220
Q_{C15}(p.u.)	0.0058	0.0289	0.0431	0.0080
Q_{C17}(p.u.)	0.0500	0.0400	0.0261	0.0250
Q_{C20}(p.u.)	0.0354	0.0368	0.0075	0.0390
Q_{C21}(p.u.)	0.0115	0.0021	0.0340	0.0270
Q_{C23}(p.u.)	0.0419	0.0426	0.0211	0.0100
Q_{C24}(p.u.)	0.0127	0.0236	0.0131	0.0170
Q_{C29}(p.u.)	0.0189	0.0105	0.0357	0.0500
F_{BF} ($/h)	872.74	873.45	**865.39**	879.91
F_{AP} (MW)	4.8843	4.6347	**4.3553**	4.2179
F_{EM} (ton/h)	0.2130	0.2137	**0.2128**	0.2165

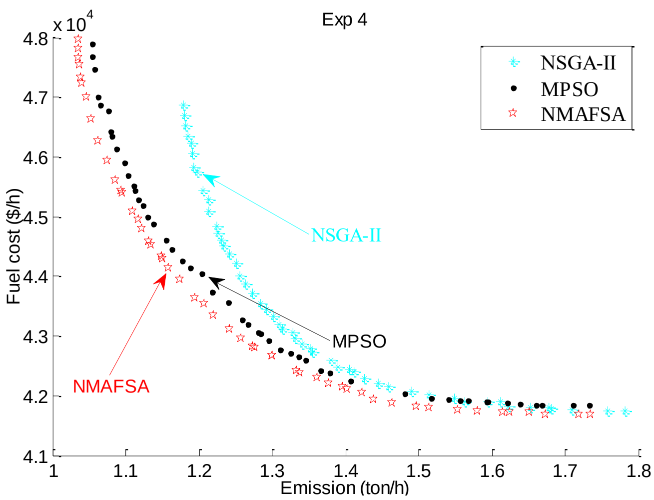

Fig.8 PFs of *Exp* 4

2) *Exp 5*

At present, there are only a few intelligent algorithms to study the triple-objective MOOPF problems on the IEEE 57-bus system. It is exciting that the NMAFSA method put forward in this paper has the potential to deal with the tri-objective optimization effectively.

Fig. 9 and Fig. 10 separately show the PF of NMAFSA algorithm compared with NSGA-II and MPSO algorithms. The diversity of PF obtained by NMAFSA clearly better than NSGA-II method, and the distribution is obviously superior to MPSO method. The control variables of BCSs found by three involved methods are listed in TABLE VI. TABLE VI states that the BCS of NMAFSA algorithm which is composed of 42605.49 of F_{BF}, 11.6947 of F_{AP} and 1.4151 of F_{EM} dominates the ones of NSGA-II and MPSO methods. Furthermore, NMAFSA algorithm also achieves the smaller F_{BF} and F_{EM} values comparing with MONBA-CPNS algorithm published in literature [22].

Exp 4 and *Exp* 5 indicate that the great advantage of NMAFSA algorithm in dealing with the non-convex MOOPF problem is more fully reflected on the larger-scale 57-bus system.

TABLE V
BCS SOLUTIONS OF *EXP* 4

independent variables	NSGA-II	MPSO	NMAFSA	MODFA [18]
P_{G2}(MW)	99.8469	96.2005	98.7165	99.9703
P_{G3}(MW)	101.5084	95.0937	90.5956	88.2975
P_{G6}(MW)	99.6098	98.1370	100.0000	99.9135
P_{G8}(MW)	287.1533	364.6798	355.8303	343.6324
P_{G9}(MW)	99.8504	100.0000	100.000	99.9138
P_{G12}(MW)	365.8721	304.5912	306.9302	310.8878
V_{G1}(p.u.)	1.0006	1.0095	1.0621	1.0600
V_{G2}(p.u.)	1.0007	0.9903	1.0553	1.0544
V_{G3}(p.u.)	1.0007	0.9858	1.0590	1.0467
V_{G6}(p.u.)	1.0007	0.9847	1.0556	1.0500
V_{G8}(p.u.)	1.0007	0.9865	1.0609	1.0558
V_{G9}(p.u.)	1.0007	0.9999	1.0497	1.0433
V_{G12}(p.u.)	1.0007	1.0146	1.0657	1.0332
T_{19}(p.u.)	0.9021	1.0814	1.0398	0.9916
T_{20}(p.u.)	1.0996	0.9113	0.9460	0.9805
T_{31}(p.u.)	1.0855	0.9814	0.9217	0.9972
T_{35}(p.u.)	0.9325	1.0263	1.0917	0.9693
T_{36}(p.u.)	0.9805	0.9383	0.9651	0.9646
T_{37}(p.u.)	1.0992	1.0709	0.9805	0.9788
T_{41}(p.u.)	0.9249	0.9378	1.0127	0.9570
T_{46}(p.u.)	1.0710	1.0254	0.9585	0.9741
T_{54}(p.u.)	1.0169	0.9000	0.9530	1.0310
T_{58}(p.u.)	0.9007	0.9084	1.0421	0.9523
T_{59}(p.u.)	0.9316	0.9843	0.9477	0.9452
T_{65}(p.u.)	1.0125	1.0461	1.0001	1.0045
T_{66}(p.u.)	0.9002	0.9473	0.9516	0.9344
T_{71}(p.u.)	0.9567	0.9937	0.9295	0.9481
T_{73}(p.u.)	1.0657	0.9313	0.9800	0.9621
T_{76}(p.u.)	0.9018	0.9720	0.9786	0.9587
T_{80}(p.u.)	0.9143	1.0350	1.0218	0.9703
Q_{C18}(p.u.)	0.2026	0.0000	0.0254	0.1896
Q_{C25}(p.u.)	0.1233	0.2104	0.2296	0.1191
Q_{C53}(p.u.)	0.2773	0.1487	0.0539	0.0331
F_{BF} ($/h)	43876.06	43278.28	**43114.71**	43174.57
F_{EM} (ton/h)	1.2643	1.2585	**1.2421**	1.2679

TABLE VI
BCS SOLUTIONS OF *EXP* 5

independent variables	NSGA-II	MPSO	NMAFSA	MONBA-CPNS [22]
P_{G2}(MW)	97.3371	69.4687	88.0998	99.1093
P_{G3}(MW)	96.5188	89.7803	85.6876	97.7004
P_{G6}(MW)	90.5771	91.7003	93.2268	89.4406
P_{G8}(MW)	319.1209	356.6882	345.1766	312.8840
P_{G9}(MW)	81.6383	98.4973	89.7787	98.3716
P_{G12}(MW)	402.1791	365.8965	375.3263	404.5135
V_{G1}(p.u.)	1.1000	1.1000	1.1000	1.0940
V_{G2}(p.u.)	1.1000	1.0972	1.1000	1.0894
V_{G3}(p.u.)	1.1000	1.0929	1.1000	1.0883
V_{G6}(p.u.)	1.1000	1.0986	1.1000	1.0961
V_{G8}(p.u.)	1.1000	1.1000	1.1000	1.0980
V_{G9}(p.u.)	1.0999	1.0886	1.1000	1.0893
V_{G12}(p.u.)	1.1000	1.0796	1.1000	1.0830
T_{19}(p.u.)	1.0566	1.0452	1.0769	0.9756
T_{20}(p.u.)	0.9837	1.0491	0.9953	1.0194
T_{31}(p.u.)	1.0129	1.0873	0.9903	0.9533
T_{35}(p.u.)	1.0823	1.0501	1.0716	1.1000
T_{36}(p.u.)	1.0965	1.0250	1.0914	1.0631
T_{37}(p.u.)	1.0866	0.9953	1.0617	0.9934
T_{41}(p.u.)	1.0806	1.0954	1.0794	1.0238
T_{46}(p.u.)	1.0275	0.9764	1.0007	0.9594
T_{54}(p.u.)	1.0998	0.9333	1.0962	0.9938
T_{58}(p.u.)	0.9861	1.0182	0.9923	0.9738
T_{59}(p.u.)	1.0384	1.0286	0.9875	0.9791
T_{65}(p.u.)	0.9834	1.0092	1.0062	0.9907
T_{66}(p.u.)	1.0687	1.0070	0.9584	0.9709
T_{71}(p.u.)	0.9678	1.0447	0.9821	1.0038
T_{73}(p.u.)	1.0796	0.9708	1.0837	1.0997
T_{76}(p.u.)	0.9396	0.9983	0.9487	0.9763
T_{80}(p.u.)	1.0578	1.0768	1.0897	1.0077
Q_{C18}(p.u.)	0.0665	0.1633	0.1230	0.1225
Q_{C25}(p.u.)	0.2795	0.1959	0.2236	0.2179
Q_{C53}(p.u.)	0.2617	0.1385	0.1767	0.1676
F_{BF} ($/h)	43119.96	42668.69	**42605.49**	43052.18
F_{AP} (MW)	12.6817	12.1123	**11.6947**	10.5961
F_{EM} (ton/h)	1.4429	1.4248	**1.4151**	1.4292

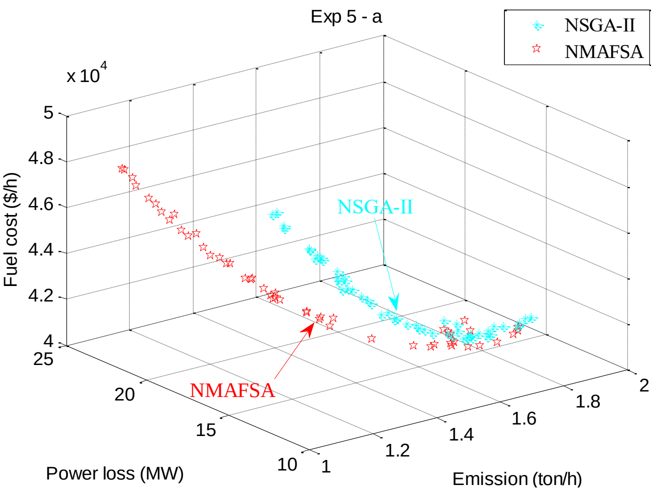

Fig.9 PFs of NSGA-II and NMAFSA for *Exp* 5

C. *Trials on IEEE 118-bus System*

A dual-objective case (*Exp* 6) which aims to reduce F_{BF} and F_{EM} concurrently is performed on the complex IEEE 118-bus system. The PFs and the specific solutions of *Exp* 6, respectively, are given in Fig. 11 and TABLE VII. Fig. 11 intuitively shows that the PF found by MPSO is much more irregularly-distributed and the PF of NMAFSA is clearly advantageous to NSGA-II method.

The BCS, the boundary solution with minimal F_{BF} and the boundary one with minimal F_{EM} are given in TABLE VII. Specifically, the BCS of NMAFSA including 61719.19 of F_{BF} and 2.3569 of F_{EM} is more preferable than the BCSs of NSGA-II and MPSO algorithms. Furthermore, the NMAFSA algorithm put forward in this paper achieves 60144.08 of minimal F_{BF} and 2.1024 of minimal F_{EM}.

TABLE VII
SPECIFIC SOLUTIONS OF *EXP* 6

Exp 6		NSGA-II	MPSO	NMAFSA
BCS	F_{BF}	61738.97	61849.58	**61719.19**
	F_{EM}	2.6834	2.6965	**2.3569**
minimal F_{BF}	F_{BF}	60784.76	60489.66	**60144.08**
	F_{EM}	3.3625	3.3914	3.0520
minimal F_{EM}	F_{BF}	64280.06	62841.95	63863.76
	F_{EM}	2.2770	2.3950	**2.1024**

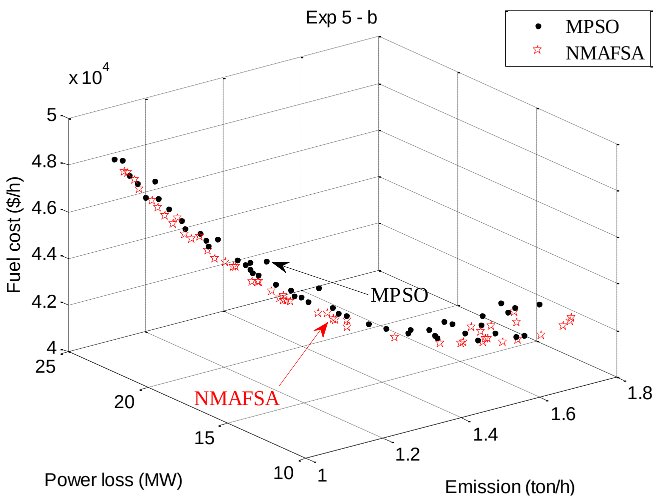

Fig.10 PFs of MPSO and NMAFSA for *Exp* 5

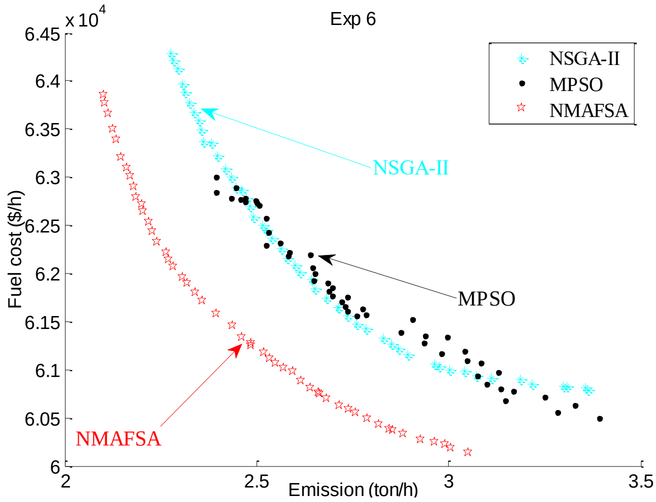

Fig.11 PFs of *Exp* 6

VI. Evaluation

In this paper, the convergence and distribution of PFs obtained by NMAFSA algorithm are discussed based on the iterative process and generation distance (GD) index.

A. Convergence

Taking the *Exp* 1 as an example, the convergence of three mentioned algorithms is analyzed from the dynamic iterative process. Fig. 12 shows the iterative process of NMAFSA, MPSO and NSGA-II methods. It is not difficult to find that, the presented NMAFSA algorithm seeks the qualified POS which satisfies all *ER*s and *IR*s at the 57th iteration. The NSGA-II and MPSO find the POS with zero constraint violation at the 86th and 128th iterations, respectively. Thus, Fig. 12 proves the superiority of NMAFSA algorithm in fast convergence.

B. Distribution

The distribution of obtained POS for four dual-objective trials in this paper (*Exp*s 1, 2, 4, 6) is analyzed quantitatively based on GD index. The GD index is expressed as formula (27) and its definition can be found in [18, 21, 29].

$$GD = \sqrt{\sum_{i=1}^{N} de_i^2} \Big/ N \tag{27}$$

The smaller GD value represents the better distribution of obtained POS. The boxplots and average values of GD index for all dual-objective trials are shown in Fig. 13 and TABLE VIII. The closer boxplots and smaller average of GD index indicate that the PF of NMAFSA algorithm is more consistent with the reference PF. The smaller deviation values also validate that compared with MPSO and NSGA-II algorithms, NMAFSA algorithm achieves the more stable operation.

TABLE VIII
AVERAGE AND DEVIATION OF GD

GD		NSGA-II	MPSO	NMAFSA
Exp 1	average	0.1522	0.1918	0.1341
	standard deviation	0.0310	0.0944	0.0263
Exp 2	average	0.1676	0.1742	0.1663
	standard deviation	0.0331	0.0496	0.0327
Exp 4	average	0.7688	0.9858	0.7359
	standard deviation	0.1533	0.2507	0.1466
Exp 6	average	1.9111	5.1799	1.8138
	standard deviation	0.8159	3.1270	0.6765

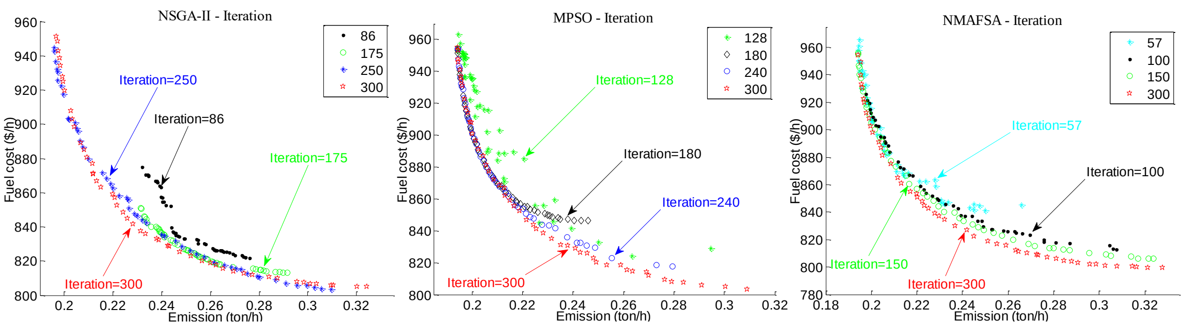

Fig.12 Iterative process of *Exp* 1

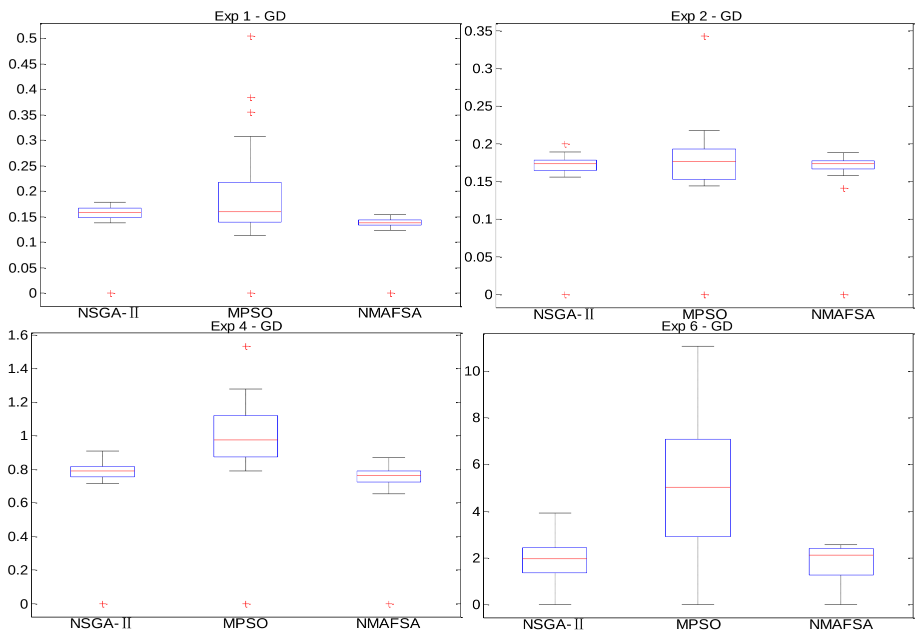

Fig.13 Boxplot of GD index for dual-objective cases

VII. Conclusion

The optimized operation of electric system, one of the most common practical engineering problems, has been widely concerned. In this paper, the novel NMAFSA algorithm with OSG guidance and NIR retention mechanisms is proposed to solve the complex MOOPF problems. Six dual-goal and triple-goal MOOPF trials on three different-scale systems are carried out to demonstrate the extensive applicability of suggested NMAFSA method. Plenty of results indicate that in contrast to MPSO and NSGA-II algorithms, NMAFSA algorithm obtains the evenly-distributed PFs and the more satisfactory BCS solutions. Besides, the iterative process and GD index also prove the great edges of NMAFSA algorithm in fast-convergence and better-distribution when dealing with the high-dimensional MOOPF problems.

As the representative of solving practical engineering problems with computer technology, the NMAFSA algorithm is of great significance to deal with the security-constrained MOOPF problems more effectively.

Acknowledgements

The authors would like to thank the editors and reviewers for their constructive comments and valuable suggestions.

References

[1] T. C. Bora, V. C. Mariani and L. D. S. Coelho, "Multi-objective optimization of the environmental-economic dispatch with reinforcement learning based on non-dominated sorting genetic algorithm", *Applied Thermal Engineering*, vol. 146, pp. 688-700, 2019.

[2] H. Liang, Y. Liu, F. Li, and Y. Shen, "A multiobjective hybrid bat algorithm for combined economic/emission dispatch", *International Journal of Electrical Power and Energy Systems*, vol. 101, pp. 103-115, 2018.

[3] G. Chen, X. Yi, Z. Zhang, and S. Qiu, "Solving optimal power flow using cuckoo search algorithm with feedback control and local search mechanism", *IAENG International Journal of Computer Science*, vol. 46, no. 2. pp. 321-331, 2019.

[4] S. S. Reddy, "Solution of multi-objective optimal power flow using efficient meta-heuristic algorithm", *Electrical Engineering*, vol. 100, no. 2, pp. 401-413, 2018.

[5] G. Chen, S. Qiu, Z. Zhang, and Z. Sun, "Quasi-oppositional cuckoo search algorithm for multi-objective optimal power flow", *IAENG International Journal of Computer Science*, vol. 45, no. 2, pp. 255-266, 2018.

[6] X. Yuan, B. Zhang, P. Wang, J. Liang, Y. Yuan, Y. Huang, and X. Lei, "Multi-objective optimal power flow based on improved strength Pareto evolutionary algorithm", *Energy*, vol. 122, pp. 70-82, 2017.

[7] N. Zainal, A. M. Zain and S. Sharif, "Overview of artificial fish swarm algorithm and its applications in industrial problems", *Applied Mechanics and Materials*, vol. 815, pp. 253-257, 2015.

[8] T. Sun, H. Zhang, D. Gao, S. Liu, and Y. Cao, "Application of the artificial fish swarm algorithm to well trajectory optimization", *Chemistry and Technology of Fuels and Oils*, vol. 55, no. 2, pp, 213–218, 2019.

[9] G. Chen, J. Qian, Z. Zhang, and Z. Sun, "Multi-objective improved bat algorithm for optimizing fuel cost, emission and active power loss in power system", *IAENG International Journal of Computer Science*, vol. 46, no. 1, pp. 118-133, 2019.

[10] S. S. Reddy, "Optimal power flow using hybrid differential evolution and harmony search algorithm", *International Journal of Machine Learning and Cybernetics*, vol. 10, no. 5, pp. 1077-1091, 2019.

[11] G. Chen, J. Qian, Z. Zhang, and Z. Sun, "Applications of novel hybrid bat algorithm with constrained Pareto fuzzy dominant rule on multi-objective optimal power flow problems", *IEEE Access*, vol. 7, pp. 52060-52084, 2019.

[12] S. Rahmani and N. Amjady, "Enhanced goal attainment method for solving multi-objective security-constrained optimal power flow considering dynamic thermal rating of lines", *Applied Soft Computing*, vol. 77, pp. 41-49, 2019.

[13] C. R. E. S. Rex, M. M. Beno and J. Annrose, "Optimal power flow-based combined economic and emission dispatch problems using hybrid PSGWO algorithm", *Journal of Circuits Systems and Computers*, vol. 28, no. 9, 2019.

[14] P. P. Biswas, P. N. Suganthan, R. Mallipeddi, and G. A. J. Amaratunga, "Optimal power flow solutions using differential evolution algorithm integrated with effective constraint handling techniques", *Engineering Applications of Artificial Intelligence*, vol. 68, pp. 81-100, 2018.

[15] G. Chen, L. Liu, Z. Zhang, and S. Huang, "Optimal reactive power dispatch by improved GSA-based algorithm with the novel strategies to handle constraints", *Applied Soft Computing*, vol. 50, pp. 58-70, 2017.

[16] K. Deb, A. Pratap, S. Agarwal, and T. Meyarivan, "A fast and elitist multiobjective genetic algorithm: NSGA-II", *IEEE Transactions on Evolutionary Computation*, vol. 2, no. 6, pp. 182-197, 2002.

[17] J. Zhang, S. Wang, Q. Tang, Y. Zhou, and T. Zeng, "An improved NSGA-III integrating adaptive elimination strategy to solution of many-objective optimal power flow problems", *Energy*, vol. 172, pp. 945-957, 2019.

[18] G. Chen, X. Yi, Z. Zhang, and H. Wang, "Applications of multi-objective dimension-based firefly algorithm to optimize the power losses, emission, and cost in power systems", *Applied Soft Computing*, vol. 68, pp. 322-342, 2018.

[19] P. C. Roy, K. Deb and M. M. Islam, "An efficient nondominated sorting algorithm for large number of fronts", *IEEE Transactions on Cybernetics*, vol. 49, no. 3, pp. 859-869, 2019.

[20] H. Li, K. Deb, Q. Zhang, P. N. Suganthan, and L. Chen, "Comparison between MOEA/D and NSGA-III on a set of novel many and multi-objective benchmark problems with challenging difficulties", *Swarm and Evolutionary Computation*, vol. 46, pp. 104-117, 2019.

[21] G. Chen, J. Qian, Z. Zhang, and Z. Sun, "Multi-objective optimal power flow based on hybrid firefly-bat algorithm and constraints-prior object-fuzzy sorting strategy", *IEEE Access*, vol. 7, no. 1, pp. 139726-139745, 2019.

[22] G. Chen, J. Qian, Z. Zhang, and Z. Sun, "Many-objective new bat algorithm and constraint-priority non-inferior sorting strategy for optimal power flow", *Engineering Letters*, vol. 27, no. 4, pp. 882-892, 2019.

[23] J. Guo, J. Zhong, Y. Li, B. Du, and S. Guo, "A hybrid artificial fish swam algorithm for disassembly sequence planning considering setup time", *Assembly Automation*, vol. 39, no. 1, pp. 140-153, 2019.

[24] L. Zou, H. Li, W. Jiang, and X. Yang, "An improved fish swarm algorithm for neighborhood rough set reduction and its application", *IEEE Access*, vol. 7, pp. 90277-90288, 2019.

[25] G. Zhou, Y. Li, Y. He and X. Wang, "Artificial fish swarm based power allocation algorithm for MIMO-OFDM relay underwater acoustic communication", *IET Communications*, vol. 12, no. 9, pp. 1079-1085, 2018.

[26] G. Chen, J. Cao, Z. Zhang, and Z. Sun, "Application of imperialist competitive algorithm with its enhanced approaches for multi-objective optimal reactive power dispatch problem", *Engineering Letters*, vol. 27, no. 3, pp. 579-592, 2019.

[27] G. Chen, Z. Lu, Z. Zhang, and Z. Sun, "Research on hybrid modified cuckoo search algorithm for optimal reactive power dispatch problem ", *IAENG International Journal of Computer Science*, vol. 45, no. 2, pp. 328-339, 2018.

[28] G. Chen, X. Yi, Z. Zhang, and H. Lei, "Solving the multi-objective optimal power flow problem using the multi-objective firefly algorithm with a constraints-prior Pareto-domination approach", *Energies*, vol. 11, no. 12. pp. 3438, 2018.

[29] H. Ishibuchi, R. Imada, Y. Setoguchi, and Y. Nojima, "Reference point specification in inverted generational distance for triangular linear Pareto front", *IEEE Transactions on Evolutionary Computation*, vol. 22, no. 6, pp. 961-975, 2018.